International Journal of Pharmaceutics 361 (2008) 209–221

Contents lists available at ScienceDirect

International Journal of Pharmaceutics

journal homepage: www.elsevier.com/locate/ijpharm

Pharmaceutical Nanotechnology

The surface characterisation and comparison of two potential sub-micron, sugar bulking excipients for use in low-dose, suspension formulations in metered dose inhalers

Jeff James [a,*], Barry Crean [a], Martyn Davies [a], Richard Toon [b], Phil Jinks [b], Clive J. Roberts [a]

[a] Laboratory of Biophysics and Surface Analysis, School of Pharmacy, The University of Nottingham, Nottingham NG7 2RD, UK
[b] 3M Health Care Ltd., 1 Morley Street, Loughborough, Leicestershire LE11 1EP, UK

ARTICLE INFO

Article history:
Received 23 August 2007
Received in revised form 3 May 2008
Accepted 23 May 2008
Available online 4 June 2008

Keywords:
Pressurised metered dose inhalers (pMDIs)
Atomic force microscopy (AFM)
Surface free energy
Lactose and sucrose
Active pharmaceutical ingredients (APIs)
Bulking excipients

ABSTRACT

Purpose: This study compares the surface characteristics and surface energetics of two potential bulking excipients, anhydrous sub-micron α-lactose and sub-micron sucrose, for use with low-dose, suspension formulations in pressurised metered dose inhalers (pMDIs). Both sub-micron bulking excipients are processed from parent materials (α-lactose monohydrate/α-lactose monohydrate and silk grade sucrose, respectively) so the surface characteristics of each material were determined and compared. Additionally, the surface energetics and adhesive interactions between each sub-micron bulking excipient and some chosen active pharmaceutical ingredients (APIs) used in pMDI formulations were also determined. From this data, it was possible to predict the potential degree of interaction between the APIs and each sub-micron bulking excipient, thus determining suitable API–excipient combinations for pMDI formulation optimisation. Salmon calcitonin was also investigated as a potential API due to the current interest in, and the potential low-dose requirements for, the pulmonary delivery of proteins.
Methods: The size and morphology of each sub-micron excipient (and parent materials) were determined using scanning electron microscopy (SEM) and the crystalline nature of each sub-micron excipient and parent material was assessed using X-ray diffraction (XRD). The surface chemistry of each sub-micron excipient was analysed using X-ray photoelectron spectroscopy (XPS). The surface energies of each sub-micron excipient, along with their respective parent materials and any intermediates, were determined using two techniques. The surface energies of these materials were determined via (a) single particle adhesive interactions using atomic force microscopy (AFM) and (b) 'bulk' material surface interactions using contact angle measurements (CA). From the CA data, it was possible to calculate the theoretical work of adhesion values for each API–excipient interaction using the surface component analysis (SCA). The Young's modulus for each sub-micron excipient and parent material was also determined using AFM. Finally, the adhesive interactions were determined between each sub-micron bulking excipient and five APIs (formoterol fumarate, salmeterol xinafoate, salbutamol sulphate, mometasone furoate and salmon calcitonin).
Results: Both sub-micron sucrose and anhydrous sub-micron α-lactose exhibited a lower surface free energy than their respective parent materials/intermediates. In addition, both AFM and CA surface energy measurements also showed that sub-micron sucrose has a higher surface energy than anhydrous sub-micron α-lactose. Theoretical work of adhesion values between anhydrous sub-micron α-lactose and each API are considerably lower than those observed between micronised α-lactose monohydrate and each API. Corresponding theoretical work of adhesion values between sub-micron sucrose and each API were almost identical to those observed between silk grade sucrose and each API. Young's modulus determination revealed that sub-micron sucrose has a greater crystal hardness/elasticity ratio than anhydrous sub-micron α-lactose. With the exception of salmon calcitonin, sub-micron sucrose showed larger adhesive interactions to the selected APIs than anhydrous sub-micron α-lactose.
Conclusions: Anhydrous sub-micron α-lactose has been found to have lower adhesive interactions with a range of chosen, low-dose APIs compared to sub-micron sucrose. This could be related to the lower surface energy for anhydrous sub-micron α-lactose. Knowledge of the surface free energy and mechanical

* Corresponding author.
E-mail addresses: paxjj@nottingham.ac.uk (J. James), rtoon@mmm.com (R. Toon), clive.roberts@nottingham.ac.uk (C.J. Roberts).

0378-5173/$ – see front matter
doi:10.1016/j.ijpharm.2008.05.032

properties of potential sub-micron bulking excipients and API materials could provide useful information regarding the selection of suitable API-submicron bulking excipient combinations during the development and optimisation stages of suspension pMDI formulations.

1. Introduction

Pressurised metered dose inhalers (pMDIs) are commonly used for the treatment of various pulmonary disorders, such as asthma and chronic obstructive pulmonary disease (COPD) (Rang and Dale, 1995). There are several reasons for such favourability, e.g. the rapid onset of action via the pulmonary route (Dalby and Suman, 2003). Both solution and suspension-based pMDIs contain the active pharmaceutical ingredient (API) in a hydrofluoroalkane (HFA) propellant, possibly in the presence of co-solvents and surfactants (Smyth, 2003).

The use of potent, long acting bronchodilators, such as salmeterol xinafoate (typically 25 μg per actuation) and formoterol fumarate (typically 6 μ per actuation) in pMDI formulations has been of great therapeutic benefit to the patient. However, low-dose suspension formulations can be problematic. Large variations in the delivered dose can be observed for such low-dose formulations (Jinks, 2003). The use of bulking excipients to aid this dose variability problem in pMDI systems had, until recently, never been exploited to any great extent (Jinks, 2003). Typical excipients used in inhalation formulations for example, α-lactose monohydrate, have proven impractical for use as bulking excipients in pMDI systems, due to their particle size incompatibility with pMDI valve components. In addition, micronised versions of these excipients have also yielded poor dose uniformity results despite their reduced particle size. It is well known that micronisation can form high energy amorphous regions on the surfaces of particulates (Buckton, 1995; Feeley et al., 1998; Michael et al., 2001) and these high energy regions may have a detrimental effect on formulation stability. However, the advent of anhydrous sub-micron α-lactose as a bulking excipient, via high-pressure homogenisation, provides a promising alternative bulking excipient for use in suspension pMDI systems. This excipient is a sub-micron dispersion of anhydrous α-lactose in ethanol, prepared by the high-pressure homogenisation of micronised α-lactose monohydrate in the presence of ethanol. When incorporated with a highly potent API in a suspension pMDI formulation, the anhydrous sub-micron α-lactose appears to considerably improve dose uniformity throughout the 120-shot lifetime of the device. This is illustrated in Fig. 1 (Jinks, 2003).

Following favourable dose uniformity results with anhydrous sub-micron α-lactose, a sub-micron dispersion of sucrose was also produced as a possible alternative to lactose. Sub-micron sucrose is prepared by high-pressure homogenisation in a similar way to anhydrous sub-micron α-lactose. However, sucrose has a more rigid crystalline structure and therefore, requires multiple passes through the high-pressure homogeniser in order to obtain the required sub-micron size (Vatsaraj et al., 2003).

As novel bulking excipients are produced from parent materials via high energy, high stress processes, it is advantageous to characterise the surfaces of anhydrous sub-micron α-lactose and sub-micron sucrose. This would allow the user to gain a better understanding of the physical and chemical nature of the surfaces of these products. This in turn may aid the formulation scientist in selecting the correct API–sub-micron bulking excipient combination in order to optimise the aerosolisation performance of a given pMDI formulation. Surface characterisation methods have recently been employed to understand the surface properties of APIs and components within an inhaled delivery system (Briggs and Grant, 2003; Buckton, 1997; Sindel and Zimmerman, 2001; Tong et al., 2002). These studies have been undertaken with a view to optimising device performance by examining characteristics which are not captured by compendial testing (U.S. Pharmacopeia, 2005; European Pharmacopeia, 2002). For example, recent interest has focused on techniques such as atomic force microscopy (AFM), which can be used to directly quantify interactive force measurements for particulate APIs (e.g. Ashayer et al., 2004; Davies et al., 2005; Tsukada et al., 2004). Indeed, AFM has already been used to directly quantify certain force interactions in model pMDI systems (Ashayer et al., 2004; Traini et al., 2006). Additionally, the surface energetics of APIs have been quantified using AFM, which allows the user to determine these values via force measurements taken from isolated crystalline faces (Zhang et al., 2006). This acts as an alternative to the 'bulk' surface analysis of APIs via techniques such as inverse gas chromatography (IGC) (e.g. Columbano et al., 2003; Tong et al., 2006) and contact angle measurements (Planinsek et al., 2001; Traini et al., 2005). The studies referenced above, go some way towards illustrating how several laboratories have attempted to gain an insight into aspects of formulation stability and performance using surface analysis techniques.

This study aims to determine the surface characteristics and surface energetics of both anhydrous sub-micron α-lactose and sub-micron sucrose. The sub-micron excipients will be compared to their respective parent materials, as well as each other. In addition, the adhesive interactions between each sub-micron excipient and a selection of APIs will be determined in order to assess their suitability as bulking excipients for each API.

2. Materials and methods

2.1. API materials used in the study

Salbutamol sulphate and salmon calcitonin were supplied by 3M Drug Delivery (Loughborough, UK). Mometasone furoate was supplied by Euroasian Chemicals Pvt. Ltd. (Mumbai, India). Formoterol fumarate and salmeterol xinafoate were supplied by Sigma–Aldrich (Gillingham, UK).

2.2. Preparation of anhydrous sub-micron α-lactose and anhydrous sub-micron sucrose

Anhydrous sub-micron α-lactose and sub-micron sucrose were kindly prepared by representatives at 3M Drug Delivery (Loughborough, UK). An overview of the preparation methods is given below.

Alpha lactose monohydrate (DMV, Veghel, The Netherlands) was micronised using an APTM Superjet Kompak-2/C® 8 in. micronisер (Lugano-Stabio, Switzerland). The feed rate for this process was 4 ± 0.3 kg/h. The resultant micronised material (100 g) was then dispersed in anhydrous ethanol (840 g) using a Silverson® high shear mixer (Chesham, UK). Subsequently, the dispersion product was added to an Avestin Emulsiflex C50® homogenizer (Ottawa, Canada), where it was re-circulated at 10,000 psi processing pressure for 20 min. Following recirculation, the dispersions were then processed in a final pass at 20,000 psi.

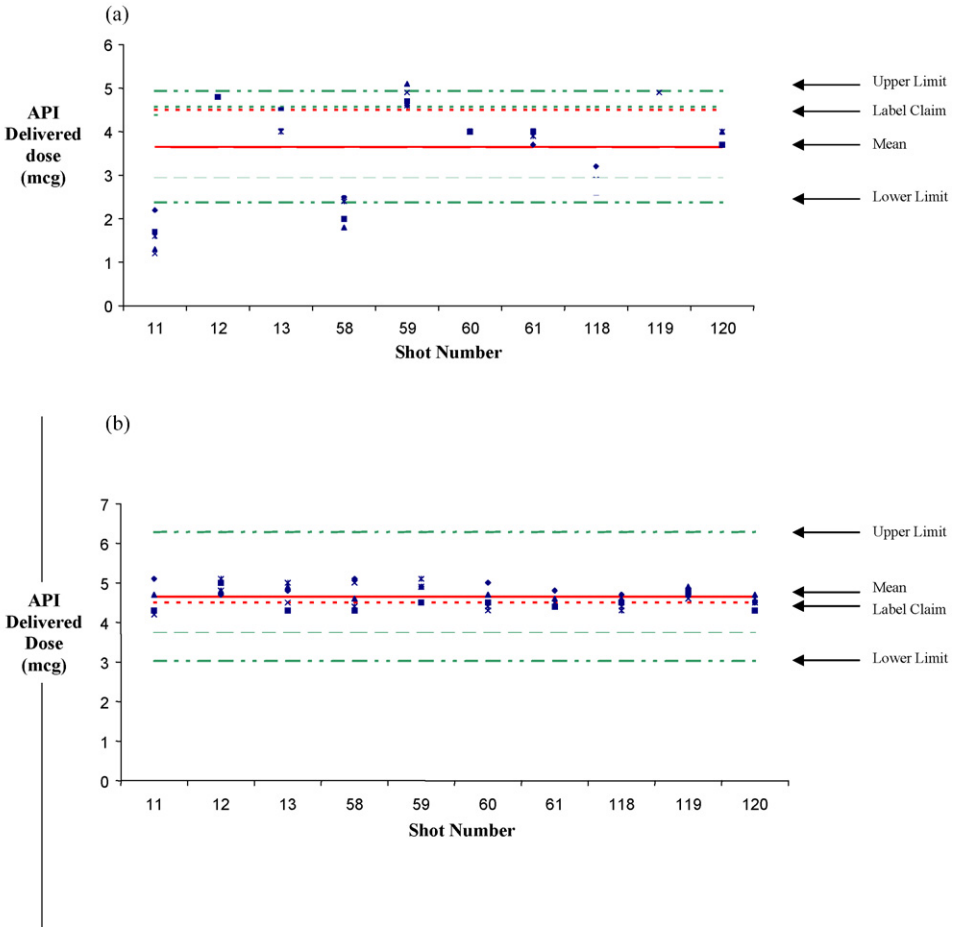

Fig. 1. Through-life dose uniformity performance of a beta agonist-HFA pMDI system (a) without anhydrous sub-micron α-lactose and (b) pMDI system with anhydrous sub-micron α-lactose (10:1 excipient–API ratio). $N = 3$ devices tested (adapted from Jinks, 2003).

Sucrose (silk grade sugar, ex BSC-3M Pharmaceuticals, Loughborough, UK) (20 g) was dispersed in dehydrated ethanol (400 g) for 1 min using a Silverson high shear stirrer. The dispersion was then processed by high-pressure homogenisation at a pressure of 25,000 psi for 60 min using a Microfluidizer M110EH (Newton, MA, USA) with a "Z" interaction chamber, in recirculation mode.

The resultant sub-micron products exist as ethanolic slurries. Powder forms of anhydrous sub-micron α-lactose and sub-micron sucrose were prepared by drying the ethanolic, anhydrous sub-micron slurries under a vacuum before storing them in vacuum desiccators. At the production site, both anhydrous sub-micron α-lactose and sub-micron sucrose underwent further chemical and physical characterisation in order to confirm the nature and sub-micron particle size of each material.

2.3. Scanning electron microscopy (SEM)

Both sub-micron bulking excipients were examined using SEM in order to characterise particle size and morphology. Prior to analysis, each sample was mounted onto a carbon stub and gold-coated prior to analysis. The samples were investigated with the JEOL 6400 SEM (JEOL (UK) Ltd., Welwyn Garden City, UK), using an accelerating voltage of 10 kV and a spot size of 45 nm.

2.4. X-ray photoelectric spectroscopy (XPS)

Each sub-micron bulking excipient was analysed using XPS in order to determine elemental surface composition. Both sub-micron bulking excipients were mounted excessively onto double-sided tape and examined using an Axis-Ultra spectrometer (Kratos Analytical, Manchester, UK). The elemental compositions of each material were determined using relative sensitivity factors (empirically modified by the manufacturer) and Casa XPS peak-fitting software. The irradiating X-rays were emitted at a take-off angle of 90°.

2.5. X-ray powder diffraction (XRPD)

Both sub-micron bulking excipients, along with their unprocessed parent materials and intermediates, were analysed by XRPD in order to determine their crystalline structure. A D8 Advance® system (Bruker AXS, Madison, WI, USA) was used to identify any differences in crystalline structure between the sub-micron bulking excipients and their corresponding unprocessed materials. The experiments were carried out at a voltage of 35 kV and a current of 20 mA, using a high flux K-alpha-1 radiation source. The scan rate was 2°/min and the chart speed was 1 cm/min.

2.6. Topographical imaging of excipients and API materials

Prior to force distance data acquisition, each bulking excipient and API was topographically imaged using a Nanoscope IIIa Multi-Mode AFM (Veeco) in Tapping mode using NPS cantilevers (Veeco). This was done to determine the root mean square (RMS) roughness of each bulking excipient and API. A scan rate of 0.5 Hz was used over a 0.7 μm × 0.7 μm scan size. Three images were acquired from

each material surface and the RMS roughness was determined via the software incorporated within the AFM system.

To facilitate AFM data acquisition from each of the lactose and sucrose materials, each sample was manually prepared in a disk form by pressing the sample powders by hand very lightly onto an adhesive carbon stub (Agar Scientific, Stansted, UK). The disk formed was approximately 12 mm in diameter and 1 mm thick. Each sample was mounted vertically by inverting the stub onto the bed of powder in order to prevent the powder 'rolling' on the adhesive face of the stub. Samples were analysed as prepared. All the samples were scanned with Static Line II (Agar Scientific) to remove possible electrostatic charges before they were subjected to the force distance acquisition.

2.7. AFM adhesion measurements

The interactive forces between the sub-micron excipients and chosen APIs were measured using AFM. This was performed using the colloid probe technique, where particles of each API material were attached to AFM cantilevers (FESP cantilevers; Veeco Santa Barbara, CA, USA) as described elsewhere (Davies et al., 2005; Eve et al., 2002) and challenged against the same compacts of each sub-micron bulking excipient used for the topography experiments. The spring constants for each cantilever (determined using the Sader method (Sader et al., 1995; Gibson et al., 2003)) ranged between 0.3 Nm^{-1} and 0.5 Nm^{-1}.

Three probes were prepared for each API. SEM was used to verify the correct positioning of the particle attached to the cantilever, i.e. to ensure that the attached particle was visibly proud of the cantilever tip (note: the samples were not gold coated, as this would clearly render the tips unsuitable for use). Imaging and force determination were performed using an EnviroScope AFM (Veeco) equipped with a Nanoscope IIIa controller and an environment chamber. Each of the colloid probes were imaged using a tip characterisation method described elsewhere (Hooton et al., 2004). Subsequently, one hundred force measurements were taken using each probe against the samples of anhydrous sub-micron α-lactose and sub-micron sucrose used for the topography imaging. A maximum load of 10 nN was applied to push the tips into contact with the sample surfaces. These force acquisition experiments were performed whilst fully submerged in 20 ml of a model propellant 2H, 3H decafluoropentane (mHFA) (Apollo Scientific, Stockport, UK). The determinations were conducted at 10 °C. Following the force data acquisition, the colloid probes were once again imaged using AFM to check the surface area of the probe had not dramatically changed during the force determination experiments. The force data was calculated using custom software.

2.8. Surface energy measurements

Three FESP cantilevers (Veeco) were used to determine the force of adhesion from isolated crystal faces of each sub-micron bulking excipient and API. Initially, in order to ascertain the flexibility (and hence exerted force) of each cantilever, the spring constants of these FESP cantilevers were determined using the Sader method (Sader et al., 1995). The spring constants for the FESP tips were between 2.4 Nm^{-1} and 3.3 Nm^{-1}. Each cantilever probe was cleaned before force acquisition using a UV cleaner (Bioforce Nanosciences, Ames, IA, USA) for 20 min to remove organic contaminants on the probe surface. The tip radius of each probe was characterized by tip self-imaging using a previously reported procedure described elsewhere (Hooton et al., 2004) in order to check the integrity of the tip throughout the experiment. Before the required force of adhesion data, it was also important to determine the deflection sensitivity of the cantilever. This was achieved by collecting force curves against a freshly cleaned borosilicate glass cover slip; this surface was used as a non-indenting reference to determine the deflection sensitivity of the cantilever. The borosilicate glass cover slip was cleaned, rinsed and dried using Piranha solution [a mixture of 30% H_2O_2 and 70% concentrated H_2SO_4 in water (1:4)], deionised water and nitrogen gas, respectively. Sixteen force curves were taken against this surface, at a distance of 100 nm between sampling points. When acquiring the force of adhesion data between the cantilever and the bulking excipient, one hundred force measurements were taken with each cantilever, using an EnviroScope AFM (Veeco). A maximum load of 10 nN was applied to push the tips into contact with the sample surfaces. Each test was conducted at ambient temperature (20 °C) and 0.2% relative humidity. A Triton Laboratory Instrument Control Application, Version 1.0.32 (Triton Technology, Keyworth, Nottinghamshire, UK) controlled and maintained the humidity within the chamber, again employing a distance of 100 nm between sampling points. The deflection sensitivity regime was repeated after the force of adhesion data acquisition in order to verify that the deflection sensitivity had not changed substantially during the experiment. Tip characterisation was also repeated in order to check the integrity of the tip throughout the experiment. The surface energies of the bulking excipients and APIs were determined by the known surface energy of the silica probe and the measured adhesion to each excipient (discussed further in this section).

2.9. Contact angle measurements

The contact angles of water, diiodomethane and ethylene glycol were determined against compacts of each sub-micron excipient and API material, using the sessile drop method (Kwok et al., 1998). Results were obtained using a DSA 100 optical Contact Angle meter (KSV Instruments, Helsinki, Finland) at ambient conditions. Using a micro-syringe, a drop of pure-deionised water (~60 μl) was dispensed onto the surface of each API. The contact angle of the drop was recorded at 0.01 s intervals using the internal high-speed camera, and the contact angles observed during this time period were determined by the software incorporated within the system. Measurements were made on five different areas for each sample. On completion, the dispersive and polar surface energy were determined using a custom built spreadsheet.

Ideally, the facilitation of contact angle measurements requires flat surfaces and therefore, each sub-micron excipient was pressed into a compact disk using the Specac Model 21050 servo-hydraulic press (Specac), pressed from 150 mg of powder for 15 min at 10 kN. The resultant compacts were stored in a tightly sealed container in a clean, dry environment for at least 24 h prior to use.

2.10. Young's modulus AFM determination

The Young's modulus of each sub-micron bulking excipients, unprocessed materials and intermediates were measured using AFM to determine the hardness/elasticity ratio of each material. Three OTESP cantilevers (Olympus, Japan) were employed for this experiment. Due to their more robust nature; the spring constants for these cantilevers ranged between 36 Nm^{-1} and 41 Nm^{-1}. Prior to data acquisition, silicon was used as a non-indenting reference needed to produce the accurate force displacement parameter (Davies et al., 2005). One hundred force measurements were recorded from each sub-micron bulking excipient, over a 10 μm × 10 μm area. The optical alignment was unchanged throughout each experiment. Each cantilever was imaged using AFM and SEM before and after force data acquisition, in order to quantify any changes in tip radius throughout the experiment.

2.11. Calculation of results

2.11.1. RMS roughness determination

The RMS roughness of each surface was determined from the topographical AFM images. This parameter was calculated using software incorporated in the AFM system, via the following equation:

$$R_{\mathrm{rms}} = \sqrt{\frac{1}{n}\sum_{i=1}^{n} y_i^2} \quad (1)$$

where n is the number of points in the topography profile, i is the asperities and y_i is the distance between the asperities.

2.11.2. AFM work of adhesion and surface energy determination

The force of adhesion (F_{adh}) between each probe and the substrates was determined using AFM. From these results, the work of adhesion (W_{A}) was calculated using the formula.

$$W_{\mathrm{A}} = \frac{3F_{\mathrm{adh}}}{2\pi R} \quad (2)$$

In this formula, R is equal to the radius of the hemispherical point of contact (assumed in accordance with the Johnson–Kendall–Roberts theory) determined by tip characterisation. Subsequently the surface free energy of material was calculated using the formula:

$$\gamma_1 = \frac{W_{\mathrm{A}}^2}{4\gamma_2} \quad (3)$$

In this equation, γ_2 relates to the surface free energy of the silicon tip, which has a nominal value of 42 mJ m^{-2}. A number of published works have shown that the dispersive surface energy of silica determined using the contact angle technique, ranged from approximately 41 mJ m^{-2} to 43 mJ m^{-2} (Ashayer et al., 2004; Davies et al., 2005). The γ_2 for silica was therefore taken to be 42 mJ m^{-2} for the purpose of this study. The sample surface deformation (d) due to indentation was calculated from the difference in the gradient of the force–distance approach curve, subsequent to contact between the reference and sample surfaces.

2.11.3. Contact angle-derived surface energy determination

The dispersive and polar surface energy determination via contact angle measurements was performed using a custom built spreadsheet based on the work of Van Oss, detailed elsewhere (Van Oss et al., 1987; Greiveldinger and Shanahan, 1999). The values were calculated using the following equation:

$$(1+\mathrm{Cos}\,\theta)\gamma_{\mathrm{L}} = 2\left(\sqrt{\gamma_{\mathrm{S}}^{\mathrm{LW}}\gamma_{\mathrm{L}}^{\mathrm{LW}}} + \sqrt{\gamma_{\mathrm{S}}^{+}\gamma_{\mathrm{L}}^{-}} - \sqrt{\gamma_{\mathrm{S}}^{-}\gamma_{\mathrm{L}}^{+}}\right) \quad (4)$$

where γ_{L} is the surface tension of the test liquid. Also, $\gamma_{\mathrm{S}}^{\mathrm{LW}}$ and $\gamma_{\mathrm{L}}^{\mathrm{LW}}$ are the dispersive Lifshitz component of surface energy for the test solid and test liquid, respectively, whilst γ_{S}^{-}, γ_{S}^{+}, γ_{L}^{-} and γ_{L}^{+} are the polar components of surface energy for the test solid and test liquid, respectively.

2.11.4. Contact angle-derived and theoretical work of adhesion determination

If the dispersive and polar components of surface energy are known for two contacting materials in their surrounding medium, it is then possible to calculate the theoretical work of adhesion between those two materials in that particular medium. This is obtained using the surface component analysis (SCA) model), of which the full theory behind this model is detailed elsewhere (Traini et al., 2006). Therefore, upon determining the dispersive and polar components of surface energy for each bulking excipient and API material, the theoretical work of adhesion (ΔG_{132}) can be calculated between an API (say, 'material 1') and an excipient (say, 'material 2') in an apolar medium ('material 3'—where the polar γ contributions (γ^{+} and γ^{-}) both equal 0) using the equation below:

$$\Delta G_{132} = 2\left(\sqrt{\gamma_1^{\mathrm{LW}}\gamma_3^{\mathrm{LW}}} + \sqrt{\gamma_2^{\mathrm{LW}}\gamma_3^{\mathrm{LW}}} - \sqrt{\gamma_1^{\mathrm{LW}}\gamma_2^{\mathrm{LW}}} - \gamma_3^{\mathrm{LW}} - \sqrt{\gamma_1^{+}\gamma_2^{-}} - \sqrt{\gamma_1^{-}\gamma_2^{+}}\right) \quad (5)$$

Thus, the free energy of interaction for the dispersive and polar forces can be calculated if the user has a knowledge of the dispersive and polar surface energies of each solid (1 and 2) and the liquid media (3).

2.11.5. Young's modulus determination

The Young's modulus (E) was calculated using the amplified Hertz Model and this is detailed elsewhere (Davies et al., 2005). To summarise, the amplified Hertz Model is based on the principle of an elastic sphere of radius, R, deforming a planar surface by δ. The Young's modulus is calculated using the following equation:

$$E - \frac{3(1-\nu^2)k\Delta z}{4\delta^{3/2}R^{1/2}} \quad (6)$$

where ν is Poisson's ratio (taken to be 0.5), k is the cantilever spring constant cantilever, and Δz is the relative piezoelectric scanner displacement. The contact radius of the AFM tip (R) was determined using the tip characterisation method employed during the AFM surface energy experiments. The difference between the gradient of the force data on the substrate and the gradient on the hard silicon surface allows the user to determine the maximum deflection (δ) and therefore the Young's modulus (E).

3. Results

3.1. SEM imaging

Scanning electron micrographs of anhydrous sub-micron α-lactose and sub-micron sucrose, along with their parent materials, are shown in Figs. 2 and 3, respectively. Figs. 2c and 3b both confirm the sub-micron particle size of the bulking excipients. Anhydrous sub-micron α-lactose has a measured particle size of approximately 800 nm, similar to that reported elsewhere (Blatchford, 2003), whilst sub-micron sucrose has a larger particle size of approximately 900 nm. The figures also highlight the morphologies of each material. Anhydrous sub-micron α-lactose appears to have a rod-like structure, compared to the more spherical morphology of sub-micron sucrose.

3.2. X-ray photoelectric spectroscopy (XPS)

XPS was used to determine the elemental composition at the surfaces of each bulking excipient. As expected, the sub-micron materials contain carbon, hydrogen and oxygen as well as trace amounts of nitrogen and silicon (Table 1). There are minimal differences in the amount of carbon and oxygen present at the surfaces for each excipient. This may indicate slightly different functionalities at each surface. The presence of these trace elements is most likely due to the use of silica gel and nitrogen gas to preserve the anhydrous nature of the sub-micron bulking excipients during storage. However, it can be assumed that they play a negligible part in the surface characteristics of either of the sub-micron bulking excipients, due to the very low level detected. The elemental compositions are in tandem with the theoretical ratios of these elements within the two sugars (Table 1) (European Pharmacopeia, 2002).

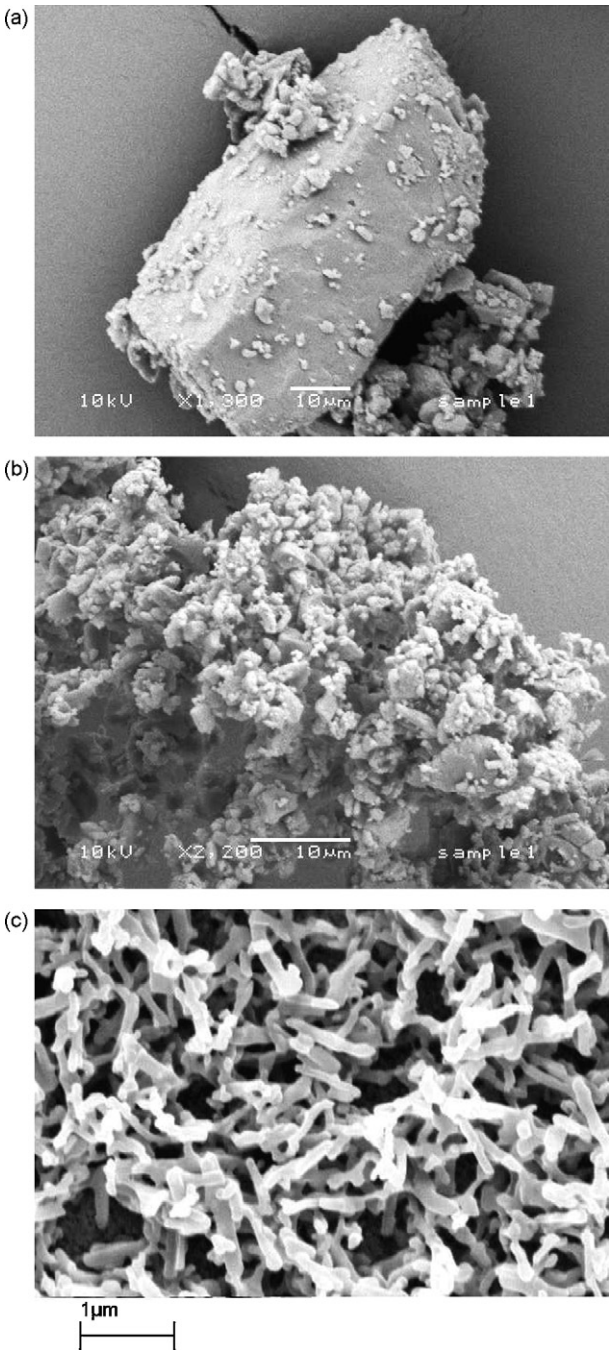

Fig. 2. SEM images of (a) α-lactose monohydrate, (b) micronised α-lactose monohydrate and (c) anhydrous sub-micron α-lactose.

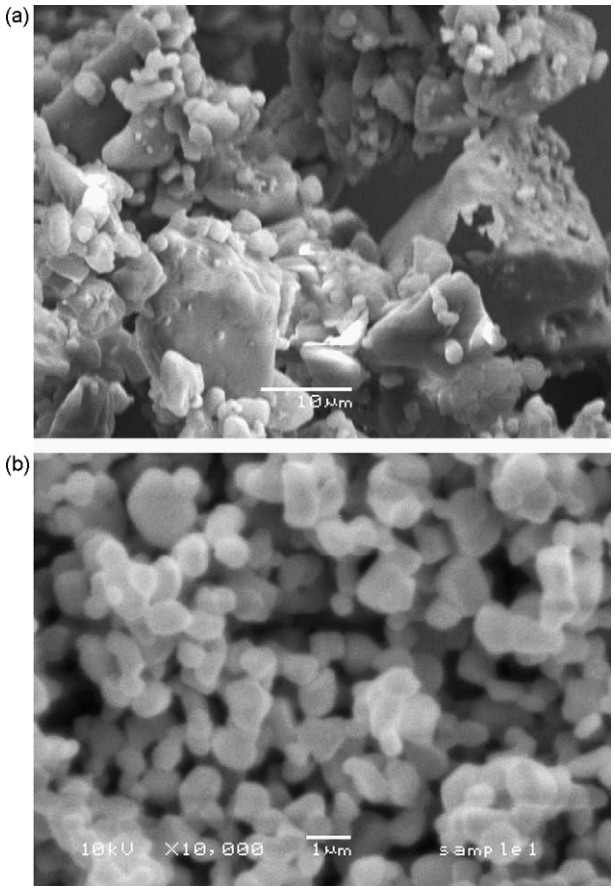

Fig. 3. SEM images of (a) silk grade sucrose and (b) sub-micron sucrose.

3.3. X-ray powder diffraction (XRPD)

The Diffrac^{Plus} SEARCH® database (Bruker) incorporated within the XRPD system was used to identify the peak positions in the data (Fig. 4). Both α-lactose monohydrate and sucrose were identified. A reference scan for anhydrous α-lactose incorporated within the database was calculated to be 98% comparable to the trace obtained for sub-micron α-lactose, thus confirming its anhydrous nature. Similarly, reference traces for α-lactose monohydrate within the database were comparable to the obtained α-lactose monohydrate and micronised α-lactose monohydrate traces, confirming the hydrated form of the unprocessed raw material and micronised intermediate. The dehydration of α-lactose monohydrate to the anhydrous form occurs during high-pressure homogenisation in ethanol. The XRPD data for sub-micron sucrose confirmed that no change in the crystal structure had occurred during the high-pressure homogenisation stage.

3.4. Topographical imaging of excipient and API materials

The mean RMS roughness of each material ($n = 3$ images) is summarised in Table 2. Meanwhile, Fig. 5 illustrates the nanoscale characterisation of FESP cantilever tips. These images demonstrate the sphere-shape of a blank tip at the nanometre scale, thus justifying the use of sphere-plane model geometry, as required by the Johnson–Kendall–Roberts method of γ determination.

Table 1
The elemental compositions of sub-micron anhydrous α-lactose and sub-micron sucrose, as determined by XPS analysis (the values in brackets denote the theoretical elemental compositions of each bulking excipient)

Elemental composition	Carbon 1s (%)	Oxygen 1s (%)	Nitrogen 1s (%)	Silicon 1s (%)
Sub-micron sucrose	52.5 (52.2)	47.3 (47.8)	0.1 (n/a)	0.1 (n/a)
Anhydrous sub-micron α-lactose	54.8 (52.2)	44.9 (47.8)	0.1 (n/a)	0.2 (n/a)

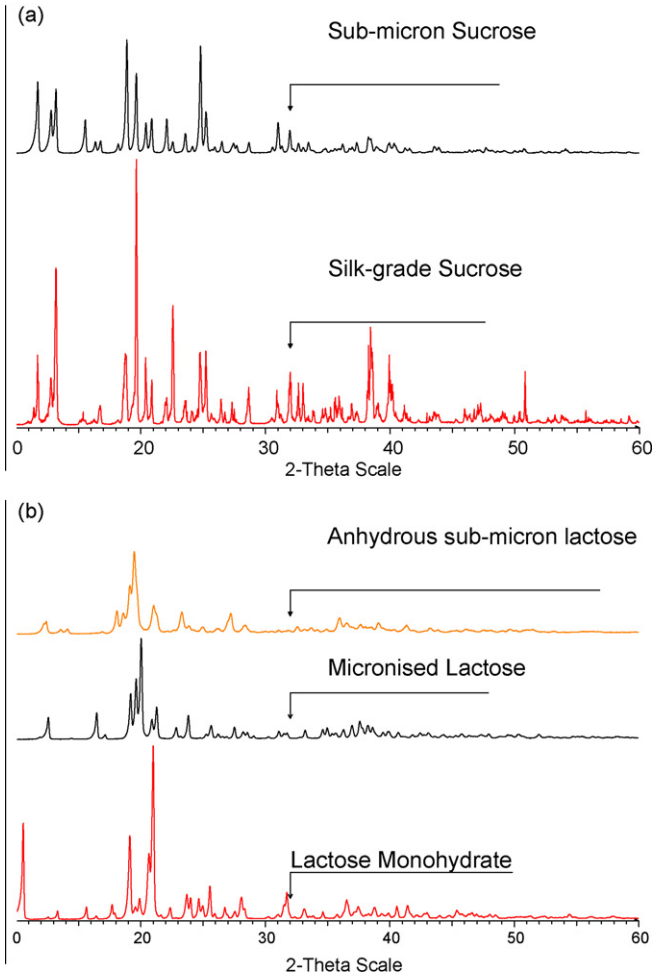

Fig. 4. Powder XRPD data comparing the crystalline structures of (a) sub-micron sucrose with silk grade sucrose and (b) anhydrous sub-micron α-lactose, to its parent materials.

3.5. AFM adhesion measurements

The mean force of adhesion measurements obtained using the colloid probes, for each of the materials, are summarised in Fig. 6. The indentations for each of the materials were recorded and are summarised in Table 2. It is clear from Fig. 6 and Table 2 that, despite similar indentation values for each sub-micron bulking excipient, there are differences in the level of adhesion to the API materials. Using a one-tailed T-test ($p < 0.05$), all of the APIs, with the exception of salmon calcitonin, exhibit significantly greater adhesion to sub-micron sucrose. There is no significant difference in the level of adhesion of salmon calcitonin between either anhydrous sub-micron α-lactose or sub-micron sucrose ($p = 0.58$).

Table 2
The mean RMS roughness and indentation values of various API materials ($n = 3 \pm$ STD)

Lactose material	Mean RMS roughness (nm)	Indentation (nm)
α-Lactose monohydrate	3.1 ± 0.7	1.2 ± 0.1
Micronised α-lactose monohydrate	4.5 ± 1.3	1.2 ± 0.1
Anhydrous sub-micron α-lactose	2.7 ± 0.4	1.0 ± 0.1
Silk grade sucrose	3.1 ± 0.7	1.7 ± 0.1
Sub-micron sucrose	7.0 ± 1.4	1.6 ± 0.1
Salmon calcitonin	1.6 ± 1.3	0.8 ± 0.0
Salmeterol xinafoate	4.2 ± 0.8	1.1 ± 0.1
Salbutamol sulphate	4.6 ± 0.3	1.0 ± 0.1
Formoterol fumarate	4.7 ± 2.1	0.9 ± 0.1
Mometasone furoate	16.6 ± 2.3	0.8 ± 0.1

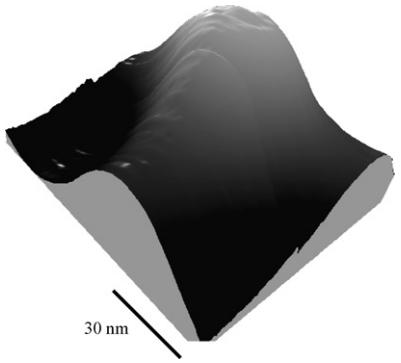

Fig. 5. A three-dimensional illustration of a FESP tip image produced using an AFM tip characterisation method.

An important consideration when obtaining adhesion measurements from a number of different surfaces is the variation in the roughness of each surface, since roughness directly affects the degree of contact between the probe and the surface. Thus, it is undesirable for the surface roughness to be a major contributing factor in the adhesion forces measured. Previous studies have shown that significant surface roughness would results in a log-normal frequency distribution of adhesive force measurements (Price et al., 2002; Young et al., 2004) whereas a smooth surface would result in a normally distributed frequency distribution of force measurements (Buckton et al., 1995; Price et al., 2002). Normal frequency distributions were obtained for all adhesion measurements; hence it can be assumed that surface roughness was not significant factor of the adhesion data produced here.

3.6. Surface energy measurements

The force of adhesion measurements obtained from each of the excipients and API materials are summarised in Table 3. The indentations depths ranged between 0.8 nm and 1.7 nm. There is

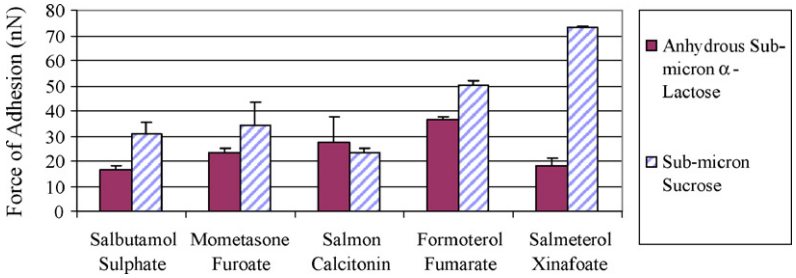

Fig. 6. Chart showing the mean relative adhesive relationships between each of the sub-micron bulking excipients, and five APIs employed in pMDI systems ($n = 3 \pm$ S.D.).

Table 3
The force of adhesion, work of adhesion and surface free energy of each lactose and sucrose excipient, and various API materials, determined using blank FESP cantilevers (3 cantilevers per material)

API/excipient	Force of adhesion (F_{ADH}) (nN)	Work of adhesion (W_A) (mJ m^{-2})	Surface energy (γ) (mJ m^{-2})
	12.9	62.0	22.0
α-Lactose monohydrate	12.5	60.8	20.1
	12.0	58.7	23.9
	11.5	94.7	53.4
Micronised α-lactose monohydrate	10.2	97.8	56.9
	12.8	91.6	49.9
	3.3	33.4	16.6
Anhydrous sub-micron α-lactose	2.9	32.7	17.5
	2.8	34.1	16.0
	48.9	110.9	77.6
Silk grade sucrose	42.4	104.0	69.7
	37.1	116.8	73.6
	23.5	82.6	47.5
Sub-micron sucrose	20.0	95.0	40.7
	26.9	89.2	54.1
	7.1	48.0	14.0
Salmon calcitonin	7.8	39.8	10.0
	6.5	56.4	18.8
	10.3	65.8	25.8
Mometasone furoate	9.2	68.9	29.2
	11.4	61.5	22.6
	10.5	58.5	28.5
Salmeterol xinafoate	10.0	55.0	26.5
	11.1	62.6	31.4
	14.8	74.9	33.4
Formoterol fumarate	14.2	77.0	35.3
	13.8	72.0	32.0
	26.3	94.1	42.4
Salbutamol sulphate	25.7	99.4	39.6
	27.3	89.8	47.0

little difference in the indentation depths for each excipient and API material. These results demonstrate that the individual surface energies of each of the API materials appear to primarily account for the differing magnitudes of the adhesion forces observed, rather than the effects of contact area. Subsequently, the indentation values were used to determine both the area of the tip at the maximum deformation of the sample. These two parameters were then used to determine the contact radii of the cantilever tips when in contact with the sample during force data acquisition. The calculated tip radii for the FESP tips were between 30 nm and 47 nm. The tip images obtained using AFM indicate that the structural integrity of each tip was uniform throughout the processes of imaging and force measurements. Thus, the validity of the results was ensured, as a significant change in tip morphology could leave the results open to variability. The frequency distribution of the measured adhesion force data was normally distributed and therefore it can again be assumed that surface roughness of each particle was not a significant influence on tip-particle adhesion.

The work of adhesion and surface energies of each sub-micron excipient are compared to the surface energies of their respective parent materials and intermediates, in Table 3. It is observed that sub-micron sucrose has a lower surface energy than silk grade sucrose. Anhydrous sub-micron α-lactose has a slightly lower surface energy than α-lactose monohydrate; and a considerably lower

Table 4
Mean dispersive and polar components of surface free energy of each lactose and sucrose excipient and various API materials, determined using contact angle measurements ($n = 3 \pm$ STD)

API/excipient	Dispersive surface energy (γ^{LW}) (mJ m^{-2})	Polar positive surface energy (γ^{+}) (mJ m^{-2})	Polar negative surface energy (γ^{-}) (mJ m^{-2})
α-Lactose monohydrate	40.74 ± 1.03	0.15 ± 0.04	35.51 ± 0.81
Micronised α-lactose monohydrate	42.30 ± 0.62	4.80 ± 0.29	29.30 ± 1.11
Anhydrous sub-micron α-lactose	41.10 ± 0.23	0.70 ± 0.10	29.40 ± 0.73
Silk grade sucrose	43.20 ± 1.71	1.04 ± 0.15	51.30 ± 2.79
Sub-micron sucrose	41.01 ± 0.94	1.03 ± 0.06	49.23 ± 1.07
Salmon calcitonin	46.00 ± 0.43	7.00 ± 0.31	13.00 ± 1.37
Mometasone furoate	47.00 ± 0.40	0.10 ± 0.01	32.00 ± 2.13
Salmeterol xinafoate	37.00 ± 0.96	0.13 ± 0.03	41.80 ± 3.04
Formoterol fumarate	47.00 ± 1.72	0.11 ± 0.01	32.00 ± 2.33
Salbutamol sulphate	45.57 ± 1.94	8.91 ± 1.55	18.07 ± 1.41

Table 5a
Theoretical work of adhesion values for each API–lactose excipient interaction

MDI component	Lactose excipients; theoretical work of adhesion ($mJ\,m^{-2}$)								
	α-Lactose monohydrate			Micronised α-lactose monohydrate			Anhydrous sub-micron lactose		
	(γ^{LW})	(γ^{AB})	(γ^{TOT})	(γ^{LW})	(γ^{AB})	(γ^{TOT})	(γ^{LW})	(γ^{AB})	(γ^{TOT})
Formoterol fumarate	17.35	9.74	27.09	18.13	30.87	49.00	17.53	14.64	32.17
Salmeterol xinafoate	12.92	8.82	21.74	13.50	31.75	45.26	13.06	14.25	27.31
Salbutamol sulphate	16.52	38.89	55.42	17.27	50.94	68.21	16.70	39.48	56.18
Mometasone furoate	17.09	8.19	25.28	17.86	28.21	46.07	17.27	12.90	30.16
Salmon calcitonin	16.70	34.35	51.04	17.44	44.44	61.89	16.87	34.72	51.59

Determined via contact angle-derived surface energy values, using the SCA approach.

Table 5b
Theoretical work of adhesion values for each API–sucrose excipient interaction

MDI component	Sucrose excipients; theoretical work of adhesion ($mJ\,m^{-2}$)					
	Silk grade sucrose			Sub-micron sucrose		
	(γ^{LW})	(γ^{AB})	(γ^{TOT})	(γ^{LW})	(γ^{AB})	(γ^{TOT})
Formoterol fumarate	18.57	18.31	36.89	17.49	18.13	35.62
Salmeterol xinafoate	13.83	17.72	31.55	13.02	17.56	30.58
Salbutamol sulphate	17.69	51.43	69.12	16.65	50.52	67.17
Mometasone furoate	18.29	16.07	34.36	17.22	15.92	33.14
Salmon calcitonin	17.87	45.25	63.12	16.83	44.45	61.27

Determined via contact angle-derived surface energy values, using the SCA approach.

surface energy than the micronised α-lactose monohydrate intermediate. Sub-micron sucrose has a higher surface energy than anhydrous sub-micron α-lactose.

3.7. Contact angle measurements

The surface free energy determined using the CA sessile drop method for each of the bulking excipients and their respective parent materials, along with each API material, are summarised in Table 4. Surface energy results determined by this method allows for the distinction between the dispersive and polar components of surface energy. In the case of anhydrous sub-micron α-lactose and its parent materials, there was little difference in the dispersive surface free energies (γ^{LW}). However, there were notable variations in the electron donor (γ^{-}) and electron acceptor (γ^{+}) portions of their energy. The same phenomenon however, was not observed when comparing sucrose and sub-micron sucrose. Larger variations in dispersive surface energy were observed between the various API materials. However, once again, the main differences between them were the polar components of their surface energy.

On determination of the surface energy of each bulking excipient and API, the theoretical work of adhesion between each bulking excipient and API was calculated using the SCA approach. The results are shown in Tables 5a and 5b. From these results, it can be seen that there is little variation in the dispersive work of adhesion results for each API–excipient interaction. Conversely, there are large differences in the polar work of adhesion between each API–excipient interaction. This suggests that the total work of adhesion is considerably influenced by polar interactions for each of the interactions investigated. This claim is reinforced by the data shown in Tables 5a and 5b. For the lactose excipients, a large increase in the polar components of the work of adhesion is observed when comparing α-lactose monohydrate and micronised α-lactose monohydrate. This in turn relates to the large increase in the total work of adhesion observed. Meanwhile, there is little change in the dispersive component of the work of adhesion between the three lactose excipients and the APIs studied. The same trend is observed between the sucrose excipients and the APIs (Table 5b).

3.8. Young's modulus AFM

The Young's modulus (E) values for the sub-micron bulking excipients, parent materials and intermediates are illustrated in Fig. 7. The results show that sub-micron sucrose has a more rigid

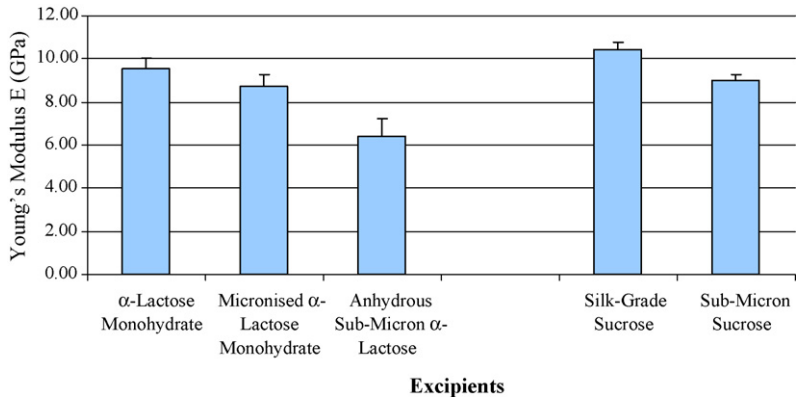

Fig. 7. Chart showing the Young's modulus of each sub-micron bulking excipient ($n = 3 \pm$ S.D.).

crystal structure than anhydrous sub-micron α-lactose. This is further supported by the indentation values obtained during these experiments; the indentation of sub-micron sucrose was 5.6 nm whereas the indentation for anhydrous sub-micron α-lactose was 6.9 nm. Hence lower indentation of sub-micron sucrose indicates that it is a more rigid crystal than anhydrous sub-micron α-lactose. Furthermore, it is interesting to note that the anhydrous sub-micron α-lactose has a less rigid crystalline structure than its micronised and unprocessed counterparts. The dehydration of α-lactose monohydrate in ethanol may cause cracks to form in the crystals which could aid the breakdown of the crystal particles during high pressure homogenisation (Garnier et al., 2002). In addition, an important determining factor for the final size of a crystal is the hardness of the material (Keck and Muller, 2006). Therefore, not only has the crystal structure of α-lactose monohydrate changed to the anhydrous form, but this conversion has produced a more compliant crystal. The Young's modulus of silk grade sucrose and sub-micron sucrose are almost identical. Since there is no dehydration step during the high-pressure homogenisation of sucrose, with a subsequent change in the unit cell of the crystal, then this further supports the suggestion that the increased crystal compliancy seen with anhydrous sub-micron α-lactose could be related to its anhydrous nature. This increase in crystal compliancy for anhydrous sub-micron α-lactose could be due to either the change in the unit cell of the α-crystalline form (i.e. the removal of water molecules from the unit cells of the α-form) or the lack of long-range order between individual α-lactose molecules due to the processing technique employed to produce them (Newell et al., 2001).

4. Discussion

The results in Table 3 show that there are distinct differences in the surface free energies of each sub-micron excipient and their respective parent and intermediate materials. This is apparent when considering the processing of anhydrous sub-micron α-lactose. As expected, the surface energy increases dramatically upon micronisation, before dropping to a similar level to α-lactose monohydrate following homogenisation. It has been suggested that during the micronisation process, the crystalline structure of α-lactose may be disrupted, thus exposing higher energy crystalline planes and potentially producing higher energy amorphous sites (Newell et al., 2001; Phillips and Byron, 1994). The consequence of exposed higher energy sites is complemented by the considerably rougher surface asperities of the micronised material, a correlation that has been previously reported by other laboratories in a range of studies using IGC and contact angle measurement (Ahfat et al., 2000; Tong et al., 2006; Buckton et al., 1988) as well as AFM measurements (Vervaet and Byron, 1999).

Whilst the conversion of α-lactose monohydrate to the sub-micron form may not be fully understood, high-pressure homogenisation of micronised α-lactose monohydrate, in the presence of anhydrous ethanol, induces dehydration and results in the production of anhydrous sub-micron particles. The surface free energy results show that the anhydrous sub-micron α-lactose crystals produced have a lower surface free energy than both α-lactose monohydrate and micronised α-lactose monohydrate. The large differences observed in the surface free energy between the different lactose materials may have a significant impact during both the manufacture and use of these materials. It is possible that high-energy sites produced during the micronisation of α-lactose monohydrate may cause particles to associate with each other during the processing of the material and also whilst the processed particles are in a suspension formulation (Tong et al., 2006; Podczeck, 1998). Therefore in this respect, the low surface free energy of anhydrous sub-micron α-lactose could make it a more promising bulking excipient than micronised α-lactose monohydrate for use in pMDI suspension formulations.

Sub-micron sucrose produced via the high-pressure homogenisation process has a lower surface free energy than silk grade sucrose, following the homogenisation process. The XRPD results in Fig. 4 indicate that the crystalline structure of sub-micron sucrose is almost identical to that of silk grade sucrose. Thus the higher surface free energy of silk grade sucrose may possibly be related to rough or amorphous regions present on the unprocessed material, in comparison to the homogenised sub-micron counterpart.

Sucrose requires many passes through a high-pressure homogeniser in order to obtain its sub-micron size. This could possibly be related to its harder crystal structure compared to that of micronised α-lactose monohydrate. In addition, sub-micron sucrose shows higher adhesive interactions with formoterol fumarate, mometasone furoate and salmeterol xinafoate. There is a significant difference between the surface free energies of the two sub-micron bulking excipients. This could be a factor, which accounts for the generally higher adhesion of sub-micron sucrose to the studied APIs.

This difference in surface free energy is somewhat surprising particularly when one considers that the two compounds have similar surface elemental composition. Silk grade sucrose undergoes much harsher processing to make sub-micron sucrose, when compared to the process of creating sub-micron lactose from α-lactose monohydrate. Thus it could be suggested that the higher surface energy of sub-micron sucrose is related to the presence of high-energy sites exposed during processing. However this may not be the case for two reasons. Firstly, silk grade sucrose has a significantly higher surface energy than α-lactose monohydrate (Table 3), and the surface energy of silk grade sucrose decreases following its conversion to sub-micron sucrose. Secondly, the XRPD data showed that the crystalline structure of sub-micron sucrose is almost identical to that of silk grade sucrose, suggesting no increase in amorphous (and potentially high-energy) content of sub-micron sucrose.

The observed difference may be possibly related to the orientation of these functional groups on the surfaces of the sub-micron materials. Whilst both materials have eight hydroxyl groups emanating from two tetrahydropyran rings, sucrose has a more compact crystalline structure, with each quartet of hydroxyl groups closer in proximity to each other. Thus, over the same area, sub-micron sucrose would have a greater concentration of hydroxyl groups than anhydrous sub-micron α-lactose. This increase in abundance of these polar functional groups may increase the prevalence of dipole–dipole (Keesom) interactions where hydroxyl groups exist on the substrate surface. If a corresponding API exhibited polar groups at its surface, then it could be assumed that a greater prevalence of hydroxyl groups at the sucrose crystal surface could possibly contribute to an increase in adhesion with the API materials, when compared to the anhydrous α-lactose excipient. This theory is consistent with the contact angle data in Fig. 8. The lower contact angle of sub-micron sucrose with water indicates a greater affinity for water in comparison to anhydrous sub-micron α-lactose. This in turn denotes a greater degree of polar interaction between water and sub-micron sucrose, which may be directly linked to the greater abundance of hydroxyl groups per unit area of surface. Salmon calcitonin is the only material which has a greater adhesive interaction with anhydrous sub-micron α-lactose compared to sub-micron sucrose. This may suggest that different mechanisms of adhesion could occur for macromolecules such as salmon calcitonin, compared to the small molecule APIs used in this study. A study in a different laboratory, examined the adhesion of proteins to solid substrates. This study demonstrated that the adhe-

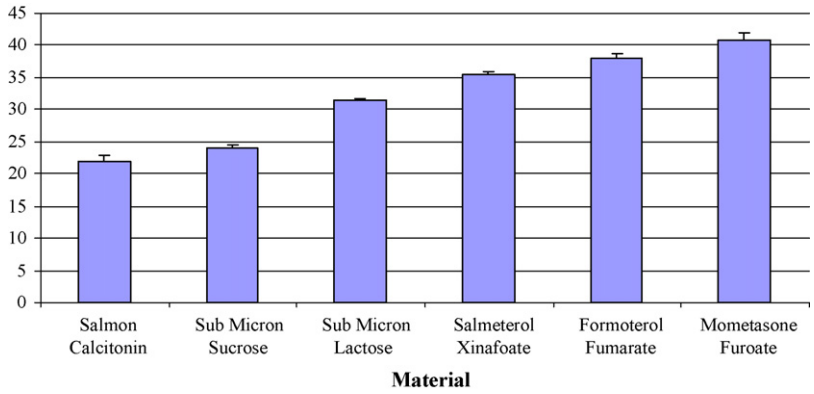

Fig. 8. Chart showing the mean water contact angle for each sub-micron bulking excipient and each API used in this experiment ($n = 5 \pm$ S.D.).

sion of proteins increases in a step-wise manner in tandem with a decrease in the wettability of the corresponding surface substrate (Sethuraman et al., 2004). Anhydrous sub-micron α-lactose has been determined to have a higher contact angle than sub-micron sucrose and therefore, is a less 'wettable' surface. Thus, using this rationale, salmon calcitonin may also interact more with the less wettable surface of anhydrous sub-micron α-lactose. Such a finding may indicate that low surface energy bulking excipients would be favourable for use in pMDI formulations incorporating proteins. However, the data in this study is limited and this should be confirmed using a number of different proteins. This is currently an area of interest in this laboratory.

From Table 4 it can be inferred that the surface energy of micronised α-lactose monohydrate is of great significance, since the polar Lewis acid/Lewis base interactions have such a great influence on the total work of adhesion. When we consider the dispersive and polar components of surface energy for the lactose excipients (Table 4) it can be seen that there is an increase in the γ^+ component for micronised α-lactose monohydrate. To aid this discussion, we must employ the arbitrary definitions of 'monopolar' and 'bipolar' materials; where for example a 'γ^- monopole' has a γ^+ surface energy component less than 1 mJ m^{-2} and a 'γ^- bipole' has a γ^+ component greater than 1 mJ m^{-2} (Van Oss et al., 1987). This means that micronised α-lactose monohydrate is bipolar, compared to α-lactose monohydrate and anhydrous sub-micron α-lactose, which are essentially monopolar. The bipolar nature of micronised α-lactose monohydrate means that there are electron-donor and electron-acceptor sites on its surface, thus allowing it to interact with both Lewis acids and Lewis bases. This is illustrated by the pronounced increase in the polar work of adhesion between micronised α-lactose monohydrate and salbutamol sulphate (Table 5a). Salbutamol sulphate is considerably bipolar since it has both a prominent γ^- and γ^+ component of surface energy (Table 4). Hence the bipolar nature of both micronised α-lactose monohydrate and salbutamol sulphate would result in a greater Lewis acid/Lewis base interaction. This results in a greater work of adhesion than that observed using α-lactose monohydrate or anhydrous sub-micron α-lactose. The same observation can be seen when considering the work of adhesion between micronised α-lactose monohydrate and salmon calcitonin (Table 5a). From these observations, it can be inferred that the bipolar nature of an excipient and an API greatly contribute to their adhesive interactions. Therefore, one could suggest that the bipolar nature of APIs and excipients (and possibly other surfaces present in a pMDI system) must be considered during pMDI API-bulking excipient formulation.

Meanwhile, the total work of adhesion between α-lactose monohydrate and each API is almost identical to that observed between anhydrous sub-micron α-lactose and each API. The same can be seen when considering silk grade sucrose and sub-micron sucrose, which supports the notion that each sub-micron excipient has very similar surface energy properties to α-lactose monohydrate and silk grade sucrose, respectively. The total work of adhesion for the sucrose excipients is generally greater than those seen for the lactose excipients, relating to the comparatively higher surface energy of the sucrose excipients.

It must be remembered that the contact angle measurements, taken from each bulking excipient and API, were acquired on powder compacts produced using a high-pressure disk press. Conversely the AFM surface energy determinations of each material were performed using the sample powder as received (i.e. no stress before analysis). Previous literature has highlighted the disruptive effects of powder compaction on the surface energy of crystalline materials (Buckton, 1995; Busignies et al., 2004a,b). Since compacts form either by brittle separation or plastic deformation (Buckton, 1995) it is highly likely that the disk press process would have disrupted the crystal structure of each material, thus exposing possible high-energy sites on the sample surface. Subsequently, it is possible that the surface energy measurements obtained from these compacts may possibly exhibit a 'higher energy bias', as a result of the compaction process. However, is has been reported that lactose forms compacts by brittle fracture and little change was found in its measured surface energy on compaction (Kiesvaara and Yliruusi, 1991). In addition, the contact angle surface energy measurements for salbutamol sulphate, formoterol fumarate and α-lactose monohydrate presented here, are comparable to results published by other laboratories (Ahfat et al., 2000; Traini et al., 2006). Nevertheless, the possible change in powder surface properties for each API and bulking excipient used in this experiment following compaction must be considered.

5. Conclusions

Both sub-micron sucrose and anhydrous sub-micron α-lactose have been characterised and compared in terms of their surface and mechanical properties. Anhydrous sub-micron α-lactose was found to have a lower surface free energy than both the α-lactose monohydrate parent material and the micronised α-lactose monohydrate intermediate. Sub-micron sucrose was also found to have a lower surface free energy than the silk grade sucrose parent material. It has been demonstrated that anhydrous sub-micron α-lactose has a much lower surface free energy than sub-micron sucrose, despite the two materials having a similar surface elemental composition. In addition, sub-micron sucrose exhibited greater levels of adhesion to a selection of APIs, when compared to anhydrous sub-micron α-

lactose. Furthermore, it has been demonstrated that sub-micron sucrose has the higher hardness/elasticity ratio of the sub-micron excipients, since it has a higher Young's modulus than anhydrous sub-micron α-lactose.

Determination of the both the theoretical and non-theoretical W_A values of both sub-micron excipients and a number of APIs could provide an indication of how each sub-micron excipient may interact with these APIs in suspension formulations. Anhydrous sub-micron α-lactose has a lower W_A value than most of the featured APIs, suggesting a lower probability of strong 'API-bulking excipient interactions'. However, sub-micron sucrose has a much higher W_A value than these APIs. This suggests that this bulking excipient could be more prone to interact with certain particulate APIs than anhydrous sub-micron α-lactose. This is confirmed by the particle–particle adhesion results that reveal that sub-micron sucrose showed greater adhesion to the chosen APIs than anhydrous sub-micron α-lactose. This is also supported by the theoretical work of adhesion values obtained for each API and excipient, again illustrating the possible differences in API–excipient adhesion. The interactions appeared to be highly dependant on the polar component of surface energy for each material. The high polar surface energy of micronised α-lactose monohydrate accounted for the large theoretical API–excipient work of adhesion values found. By comparison, anhydrous sub-micron α-lactose had a smaller polar surface energy and its resultant theoretical work of adhesion values with each API was notably smaller. This study illustrates how surface characterisation methods may aid the process of selecting suitable API–excipient combinations during pMDI formulation development.

Acknowledgements

JJ would like to thank Ms Charlotte Venus and Ms Michelle Tew for their hard work and enthusiasm in supporting aspects of this study. JJ would also like to acknowledge the efforts of Prof. Xinyong Chen, Dr Jonathon Burley and Dr Matthew Bunker (Molecular Profiles Ltd.) for their advice and support throughout this study. In addition JJ would like to thank Mr Karl Ginn (3M) and Ms Siobhan Palmer (3M) for the processing of anhydrous sub-micron α-lactose and sub-micron sucrose, respectively and Mr. Phil Jinks (3M) for supplying the in vitro data in Fig. 1. Finally, JJ thanks 3M Health Care Ltd. and the EPSRC for the funding of this studentship.

References

Ahfat, N.M., Buckton, G., Burrows, R., Ticehurst, M.D., 2000. An exploration of interrelationships between contact angle, inverse phase gas chromatography and triboelectric charging data. Eur. J. Pharm. Sci. 9, 271.

Ashayer, R., Luckham, P.F., Manimaaran, S., Rogueda, P., 2004. Investigation of the molecular interactions in a pMDI formulation by atomic force microscopy. Eur. J. Pharm. Sci. 21, 533.

Blatchford, C., 2003. Chemical and physical characterisation of sub-micron lactose, a novel bulking agent for suspension pMDI products. In: Conference Proceedings for Drug Delivery to the Lungs XIV.

Briggs, D., Grant, J., 2003. Surface Analysis by Auger and X-ray Photoelectronic Spectroscopy, First edn. IM Publications.

Buckton, G., Choularton, A., Beezer, A.E., Chatham, S.M., 1988. The effect of the comminution technique on the surface energy of a powder. Int. J. Pharm. 47, 121.

Buckton, G., 1995. Interfacial Phenomena in Drug Delivery and Targeting. Harwood Academic, Switzerland.

Buckton, G., Darcy, P., McCarthy, D., 1995. The extent of errors associated with contact angles. 3. The influence of surface-roughness effects on angles measured using a Wilhelmy plate technique for powders. Colloid Surf. A-Physicochem. Eng. Aspect 95, 27–35.

Buckton, G., 1997. Characterisation of small changes in the physical properties of powders of significance for dry powder inhaler formulations. Adv. Drug Deliv. Rev. 26, 17–27.

Busignies, V., Tchoreloff, P., Leclerc, B., Besnard, M., Couarraze, G., 2004a. Compaction of crystallographic forms of pharmaceutical granular lactoses. I. Compressibility. Eur. J. Pharm. Biopharm. 58, 569–576.

Busignies, V., Tchoreloff, P., Leclerc, B., Hersen, C., Keller, G., Couarraze, G., 2004b. Compaction of crystallographic forms of pharmaceutical granular lactoses. II. Compacts mechanical properties. Eur. J. Pharm. Biopharm. 58, 577–586.

Columbano, A., Buckton, G., Wikeley, P., 2003. Characterisation of surface modified salbutamol sulphate-alkylpolyglycoside microparticles prepared by spray drying. Int. J. Pharm. 253, 61.

Dalby, R., Suman, J., 2003. Inhalation therapy: technological milestones in asthma treatment. Adv. Drug Deliv. Rev. 55, 779.

Davies, M., Brindley, A., Chen, X.Y., Marlow, M., Doughty, S.W., Shrubb, I., Roberts, C.J., 2005. Characterization of drug particle surface energetics and Young's modulus by atomic force microscopy and inverse gas chromatography. Pharm. Res. 22, 1158–1166.

European Pharmacopeia, 2002. Section 2.9.18: Preparations for inhalation: aerodynamic assessment of fine particles. European Pharmacopeia: 4th edn., Council of Europe, 67075 Strasbourg, France.

European Pharmacopeia, 2002. European Pharmacopeia: 4th Edn, Council of Europe, 67075 Strasbourg, France.

Eve, J.K., Patel, N., Luk, S.Y., Ebbens, S.J., Roberts, C.J., 2002. A study of single drug particle adhesion interactions using atomic force microscopy. Int. J. Pharm. 238, 17–27.

Feeley, J.C., York, P., Sumby, B.S., Dicks, H., 1998. Determination of surface properties and flow characteristics of salbutamol sulphate, before and after micronisation. Int. J. Pharm. 172, 89.

Garnier, S., Petit, S., Coquerel, G., 2002. Dehydration mechanism and crystallisation behaviour of lactose. J. Therm. Anal. Calorim. 68, 489–502.

Gibson, C.T., Weeks, B.L., Abell, C., Rayment, T., Myhra, S., 2003. Calibration of AFM cantilever spring constants. Ultramicroscopy 97, 113–118.

Greiveldinger, M., Shanahan, M.E.R., 1999. A critique of the mathematical coherence of acid/base interfacial free energy theory. J. Colloid Interface Sci. 215, 170–178.

Hooton, J.C., German, C.S., Allen, S., Davies, M.C., Roberts, C.J., Tendler, S.J.B., Williams, P.M., 2004. An atomic force microscopy study of the effect of nanoscale contact geometry and surface chemistry on the adhesion of pharmaceutical particles. Pharm. Res. 21, 953–961.

Jinks, P., 2003. Preparation and utility of sub-micron lactose: a novel excipient for HFA pMDI suspensions formulations. Drug Deliv. Lungs XIV, 199–202.

Keck, C.M., Muller, R.H., 2006. Drug nanocrystals of poorly soluble drugs produced by high pressure homogenisation. Eur. J. Pharm. Biopharm. 62, 3–16.

Kiesvaara, J., Yliruusi, J., 1991. The effect of compression pressure and compression time on the surface free-energy of tablets. Acta Pharm. Nord. 3, 171–177.

Kwok, D.Y., Lam, C.N.C., Li, A., Leung, A., Wu, R., Mok, E., Neumann, A.W., 1998. Measuring and interpreting contact angles: a complex issue. Colloid Surf. A: Physicochem. Eng. Aspect 142, 219.

Michael, Y., Snowden, M.J., Chowdhry, B.Z., Ashurst, I.C., Davies-Cutting, C.J., Riley, T., 2001. Characterisation of the aggregation behaviour in a salmeterol and fluticasone propionate inhalation aerosol system. Int. J. Pharm. 221, 165.

Newell, H.E., Buckton, G., Butler, D.A., Thielmann, F., Williams, D.R., 2001. The use of inverse phase gas chromatography to measure the surface energy of crystalline, amorphous, and recently milled lactose. Pharm. Res. 18, 662–666.

Phillips, E.M., Byron, P.R., 1994. Surfactant promoted crystal growth of micronised methylprednisolone in trichloromonofluoromethane. Int. J. Pharm. 110, 9.

Planinsek, O., Trojak, A., Srcic, S., 2001. The dispersive component of the surface free energy of powders assessed using inverse gas chromatography and contact angle measurements. Int. J. Pharm. 221, 211–217.

Podczeck, F., 1998. Particle–Particle Adhesion in Pharmaceutical Powder Handling. Imperial College Press.

Price, R., Young, P.M., Edge, S., Staniforth, J.N., 2002. The influence of relative humidity on particulate interactions in carrier-based dry powder inhaler formulations. Int. J. Pharm. 246 (1–2), 47–59.

Rang, H.P., Dale, M.M., 1995. Pharmacology. Churchill Livingstone Inc., New York, NY, USA; Edinburgh, Scotland, UK, Illus. Paper.

Sader, J.E., Larson, I., Mulvaney, P., White, L.R., 1995. Method For the calibration of atomic-force microscope cantilevers. Rev. Sci. Instrum. 66, 3789–3798.

Sethuraman, A., Han, M., Kane, R.S., Belfort, G., 2004. Effect of surface wettability on the adhesion of proteins. Langmuir 20, 7779–7788.

Sindel, U., Zimmerman, I., 2001. Measurement of interaction forces between individual powder particles using an atomic force microscope. Powder Technol. 117, 247.

Smyth, H.D.C., 2003. The influence of formulation variables on the performance of alternative propellant-driven metered dose inhalers. Adv. Drug Deliv. Rev. 55, 807.

Tong, H.H.Y., Shekunov, B.Y., York, P., Chow, A.H.L., 2002. Influence of polymorphism on the surface energetics of salmeterol xinafoate crystallized from supercritical fluids. Pharm. Res. 19, 640–648.

Tong, H.H.Y., Shekunov, B.Y., York, P., Chow, A.H.L., 2006. Predicting the aerosol performance of dry powder inhalation formulations by interparticulate interaction analysis using inverse gas chromatography. J. Pharm. Sci. 95, 228.

Traini, D., Rogueda, P., Young, P., Price, R., 2005. Surface energy and interparticulate forces correlations in model pMDI formulations. Pharm. Res. 22, 816–825.

Traini, D., Young, P.M., Rogueda, P., Price, R., 2006. The use of AFM and surface energy measurements to investigate drug–canister material interactions in a model pressurized metered dose inhaler formulation. Aerosol Sci. Technol. 40, 227–236.

Tsukada, M., Irie, R., Yonemochi, Y., Noda, R., Kamiya, H., Watanabe, W., Kauppinen, E.I., 2004. Adhesion force measurement of a DPI size pharmaceutical particle by colloid probe atomic force microscopy. Powder Technol. 141, 262.

USP 28-NF 23, 2005. Chapter 601: Physical tests and determinations: Aerosols. United States Pharmacopeia. Rockville, MD, USA, pp. 2359–237.

Van Oss, C.J., Chaudhury, M.K., Good, R.J., 1987. Monopolar surfaces. Adv. Colloid Interface Sci. 28, 35–64.

Vatsaraj, N., Gao, D., Kowalski, D.L., 2003. Optimisation of the operating conditions of a lab scale Aljet mill using lactose and sucrose: a technical note. Pharm. Sci. Technol. 4, 1–6, Article 27.

Vervaet, C., Byron, P.R., 1999. Drug–surfactant–propellant interactions in HFA-formulations. Int. J. Pharm. 186, 13.

Young, P.M., Price, R., Tobyn, M.J., Buttrum, M., Dey, F., 2004. The influence of relative humidity on the cohesion properties of micronized drugs used in inhalation therapy. J. Pharm. Sci. 93, 753–761.

Zhang, J.X., Ebbens, S., Chen, X.Y., Jin, Z., Luk, S., Madden, C., Patel, N., Roberts, C.J., 2006. Determination of the surface free energy of crystalline and amorphous lactose by atomic force microscopy adhesion measurement. Pharm. Res. 23, 401–407.